Disorderless Quasi-localization of Polar Gases in One-Dimensional Lattices

Disorderless Quasi-localization of Polar Gases in One-Dimensional Lattices

W. Li,[1] A. Dhar,[1] X. Deng,[1] K. Kasamatsu,[2] L. Barbiero,[3] and L. Santos[1]
[1]Institut für Theoretische Physik, Leibniz Universität Hannover, Appelstrasse 2, 30167 Hannover, Germany
[2]Department of Physics, Kindai University, Higashi-Osaka 577-8502, Japan
[3]Center for Nonlinear Phenomena and Complex Systems, Université Libre de Bruxelles, CP 231, Campus Plaine, B-1050 Brussels, Belgium

(Received 5 February 2019; published 10 January 2020)

One-dimensional polar gases in deep optical lattices present a severely constrained dynamics due to the interplay between dipolar interactions, energy conservation, and finite bandwidth. The appearance of dynamically bound nearest-neighbor dimers enhances the role of the $1/r^3$ dipolar tail, resulting in the absence of external disorder, in quasi-localization via dimer clustering for very low densities and moderate dipole strengths. Furthermore, even weak dipoles allow for the formation of self-bound superfluid lattice droplets with a finite doping of mobile, but confined, holons. Our results, which can be extrapolated to other power-law interactions, are directly relevant for current and future lattice experiments with magnetic atoms and polar molecules.

DOI: 10.1103/PhysRevLett.124.010404

Recent years have witnessed major interest in the dynamics of isolated many-body quantum systems [1–5]. This interest has been largely triggered by impressive experimental developments, especially in cold gases [6] and trapped ions [7], which realize almost perfect isolation [8–12]. Particular attention has been paid to atom dynamics in deep optical lattices, as in seminal experiments on single-particle and many-body localization in the presence of disorder [13–18]. However, in addition to energy conservation, tight-binding dynamics in deep lattices is largely determined by the finite bandwidth. This leads to the dynamical formation of (meta)stable states. A prominent example is that of a repulsively bound pair (RBP), an on-site pair of particles that, although thermodynamically unstable, remains dynamically bound if the interaction strength exceeds the lattice bandwidth [19,20]. The presence of RBPs leads, even for weak interactions, to a strong slow-down of the dynamics [21,22].

Whereas contact-interacting particles realize Hubbard models with only on-site interactions, extended Hubbard models (EHMs) with intersite interactions may be realized using particles that interact via power-law potentials. This is the case of Rydberg atoms, with strong van der Waals interaction at nearest neighbors [23,24], and of polar lattice gases with strong dipole-dipole interactions (DDI), in particular magnetic atoms and polar molecules. Intersite spin exchange has been observed using chromium [25] and KRb [26], whereas an EHM with nearest-neighbor interactions has been realized using erbium [27]. Although EHM experiments with polar molecules remain a challenge due to inelastic losses [28,29], the latter may be avoided by using fermionic molecules [30]. In addition to leading to new ground-state physics [31,32], strong dipole-induced intersite interactions, even just between nearest neighbors, lead to nonlocal RBPs [33,34] and clusters at different sites, which significantly slow down the dynamics [35].

In this Letter, we show that the formation of dynamically bound dimers leads, in the absence of disorder, to quasi-localization for surprisingly low densities and moderate dipole strengths. Moreover, superfluid self-bound lattice droplets form even for weak dipoles [36]. Our results are directly relevant for current and future experiments on magnetic atoms and polar molecules.

Model.—We consider hard-core polar bosons in a 1D lattice [37], described by the extended Bose-Hubbard Hamiltonian (EBHM):

$$\hat{H} = -J\sum_j (\hat{a}_j^\dagger \hat{a}_{j+1} + \text{H.c.}) + \frac{V}{2}\sum_{i\neq j}\frac{1}{|i-j|^3}\hat{n}_i\hat{n}_j, \quad (1)$$

with $\hat{a}_j$ ($\hat{a}_j^\dagger$) the annihilation (creation) operator for bosons at site j, $\hat{n}_j = \hat{a}_j^\dagger\hat{a}_j$, $(\hat{a}_j^\dagger)^2 = 0$, J the hopping rate, and V the DDI between nearest neighbors [38].

Dynamically bound dimers.—For $V/J > 7$, two particles at neighboring sites form a dynamically bound nearest-neighbor dimer (NND) [39]. We first consider that all particles are paired in NNDs, which can be prepared by superimposing a superlattice on top of the primary lattice [18]. Once the NND gas is created, the superlattice is removed, and the dimers may move via second-order hopping $J_D = 8J^2/7V$ [39]. The dimer dynamics is well approximated by a dimer EBHM:

$$\frac{\hat{H}_D}{J_D} = -\sum_l (\hat{D}_l^\dagger \hat{D}_{l+1} + \text{H.c.}) + \frac{V}{J_D}\sum_{l,L\geq 1} f(L)\hat{N}_l\hat{N}_{l+L+2}, \quad (2)$$

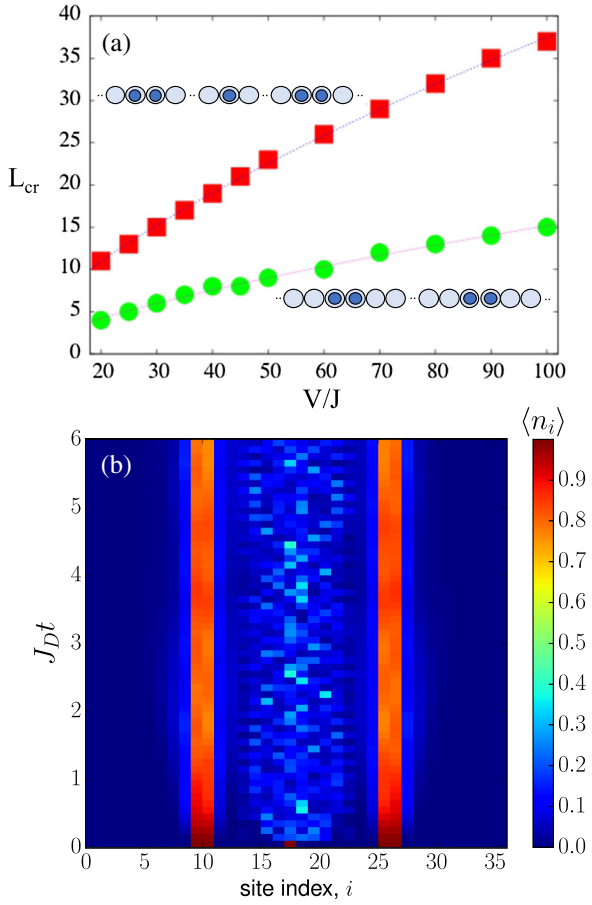

FIG. 1. (a) Squares (circles) indicate L_{cr} (see text) for two dimers with (without) a singlon in between, such that for an initial interdimer distance $L_0 < L_{cr}$ the dimers remain at a fixed distance [39]. In both cases $L_{cr} \propto (V/J)^{2/3}$ (dotted curves). (b) $\langle \hat{n}_j \rangle(t)$ evaluated by means of time-dependent density-matrix renormalization group (t-DMRG) calculations [40] using Eq. (1) for $V/J = 50$, for two dimers initially 15 sites apart and an intermediate singlon. The singlon quickly delocalizes in the interdimer space, but the dimers remain at fixed distance for $J_D t \gg 1$.

where $\hat{D}_l^\dagger = \hat{a}_l^\dagger \hat{a}_{l+1}^\dagger$ creates an NND at sites l and $l+1$, $\hat{N}_l = \hat{D}_l^\dagger \hat{D}_l$, and $f(L) = [2(L+2)^{-3} + (L+1)^{-3} + (L+3)^{-3}]$ characterizes the DDI between two dimers separated by L sites. Using $\hat{H}_D$ we determine the critical L_{cr}, such that if the initial $L_0 < L_{cr}$, then this separation remains well fixed at later times, which we quantify by imposing that the variance $\Delta L < \sqrt{L_0}$ for $J_D t = 100$ [39]. As expected from a simple inspection of $\hat{H}_D$, $L_{cr} \propto (V/J)^{2/3}$ [Fig. 1(a)].

Dimer clusters strongly slow down the dynamics, as illustrated [Fig. 2(a)] by the Shannon entropy $S(t) = -\sum_{\{n_j\}} |c(\{n_j\}, t)|^2 \log |c(\{n_j\}, t)|^2$, obtained from the state of the system $|\psi(t)\rangle = \sum_{\{n_j\}} c(\{n_j\}, t)|\{n_j\}\rangle$, with $|\{n_j\}\rangle$ Fock states characterized by occupations $n_j = 0, 1$. For $J_D t \ll 1$, $S(t)$ remains very low [41], since dimers move via second-order hopping. For $J_D t \gtrsim 1$, the dimer cluster quickly unravels for $L_0 > L_{cr}$, reaching a maximal entropy $S_{max} \simeq 2 \ln N_s$ [42]. For $L_0 < L_{cr}$, a stable dimer cluster is formed. $S(t)$ increases much slower, and only for $J_D t \gg 1$ due to the center-of-mass motion of the dimer cluster, up to $S_{max} \simeq \ln N_s$ [42].

For sufficiently large densities, clusters of more than two dimers form, strongly constraining entropy growth due to center-of-mass motion. This is illustrated in Fig. 2(b), where we depict for $V/J = 40$, the inhomogeneity parameter $\eta(t) = \sum_j |\langle \hat{n}_j \rangle - N/L|^2$ ($\eta \simeq 0$ indicates homogenization), obtained using the exact evolution of $\hat{H}_D$ for $N_D = 2$, 3, and 4 dimers initially separated by three empty sites in a lattice with $5(N_D + 1)$ sites (particle filling $\simeq 0.3$ in all cases). The homogenization time increases by 1 order of magnitude with every dimer added to the cluster. Polar dimers have hence a much stronger effect than nonpolar RBPs [43]. Whereas for the latter the larger mass of the pairs just leads to a slow-down, dimer hopping is out competed by the dipolar tail even at large distances, leading

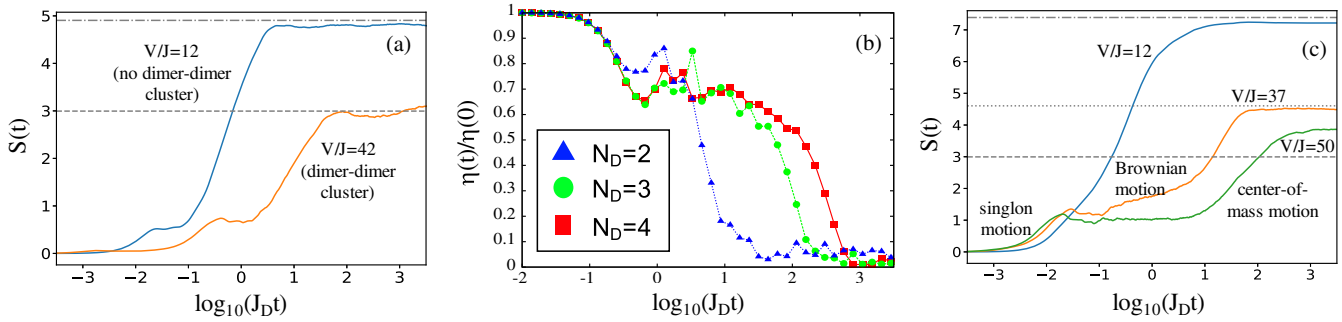

FIG. 2. (a) Shannon entropy $S(t)$, evaluated using exact evolution of Eq. (1) for 25 sites and periodic boundary conditions for two dimers initially 5 sites apart, for $V/J = 12$ (blue) and 42 (orange). Horizontal lines indicate S_{max} for unbound (dashed-dotted) and bound (dashed) dimer clusters [42]. (b) Inhomogeneity $\eta(t)/\eta(0)$ as a function of $J_D t$ evaluated using exact evolution of Eq. (2) for $V/J = 40$ for $N_D = 2$ (triangles), 3 (circles), and 4 (squares) dimers, initially with 3 sites between each dimer in a lattice with $5(N_D + 1)$ sites and periodic boundary conditions (particle filling $\simeq 0.3$). (c) Same as (a) but for two dimers initially 7 sites apart and a singlon in between for $V/J = 12$ (blue), 37 (orange), and 50 (green). Horizontal lines indicate S_{max} for dimers with an unbound relative distance (dashed-dotted), for dimers at a fixed distance with a singlon freely moving between them (dotted), and when the dimer-dimer and the dimer-singlon distance are fixed (dashed) [42].

to quasi-localization via clustering even for dilute gases and moderate dipoles [44].

Brownian motion.—Singlons (unpaired particles) radically change the dynamics. For weak-enough dipoles a singlon and a dimer can approach at one site of distance, and may resonantly swap positions, $|\ldots 1101\ldots\rangle \to |\ldots 1011\ldots\rangle$, where 0 (1) denotes an empty (occupied) site. These swaps result in dimer recoils, which induce a Brownian-like dimer motion for $Jt > 1$. In Fig. 2(c) we depict $S(t)$ for $V/J = 12$, 37, and 50 for a singlon initially between two dimers separated by 7 sites [45]. For $Jt \lesssim 1$, $S(t)$ grows due to singlon motion between dimers. For $1/J \lesssim t \lesssim 1/J_D$, Brownian motion results in an increase of $S(t)$, visible for $V/J = 37$, which is sped up by dimer hopping for $J_D t \gtrsim 1$. Being based on dimer-singlon swaps, Brownian motion is absent in a dimer gas without singlons [Fig. 2(a)], and for large V/J, [e.g., $V/J = 50$ in Fig. 2(c)] for which singlons and dimers cannot approach at one site of distance.

Singlon-gluing.—Large-enough V/J results in a dramatic singlon-induced enhancement of the interdimer binding. Because of the DDI, a singlon between two NNDs experiences a boxlike potential [39], freely moving up to a distance r_B from the dimers, with $V/r_B^3 \sim J$, fully delocalizing in a time $\sim 1/J$ over the box length $L - 2r_B$ [Fig. 1(b)]. Because of the singlon-dimer interaction, the change in singlon energy constrains the dimer motion even more strongly than the interdimer interaction. This mechanism resembles that discussed, for nonpolar gases, in Refs. [46,47], and also for polar gases in Ref. [35], in which the interplay between slow and fast particles (here dimers and singlons) was shown to result in quasi many-body localization. However, the surprisingly strong role of the DDI tail, crucial here, was overlooked in Ref. [35]. By solving a system of two dimers with an intermediate singlon [39], we confirm that $L_{\rm cr}$, which remains $\propto (V/J)^{2/3}$, is strongly enlarged [Fig. 1(a)]. For $V/J = 50$, two dimers initially $L_0 = 15$ sites apart remain at fixed distance for $J_D t \gg 1$ [Fig. 1(b)], despite the tiny interdimer DDI $Vf(L_0) \simeq 0.02J$.

Singlon-gluing crucially affects the dynamics of even dilute gases for moderate dipoles. A lattice gas at filling $\rho \ll 1$ is formed mainly by singlons, with a small dimer density $\rho_D \simeq \rho^2$ [48]. Hence, for a sufficiently large V/J that precludes Brownian motion, singlon-gluing leads to dimer clustering for $\rho \gtrsim \rho_{\rm cr} \simeq 1/\sqrt{L_{\rm cr}}$. As in the dimer gas without singlons, larger clusters of more than two dimers prevent the center-of-mass motion that results in the long-time entropy growth of Fig. 2(c). Hence even moderate DDI results for very low densities (for $V/J = 50$, $\rho_{\rm cr} \simeq 0.2$) into quasi-localization via massive dimer clustering. This estimation is conservative [48]. For lower ρ, smaller dimer clusters already constrain severely the dynamics. The required $|V|/J$ values are achievable with current state-of-the-art technology. For ^{164}Dy in an UV lattice with 180 nm spacing and depth of 23 recoil energies, $|V|/J \simeq 30$, with $J/\hbar \simeq 93\ {\rm s}^{-1}$. The dimer-hopping time is $1/J_D \simeq 280$ ms.

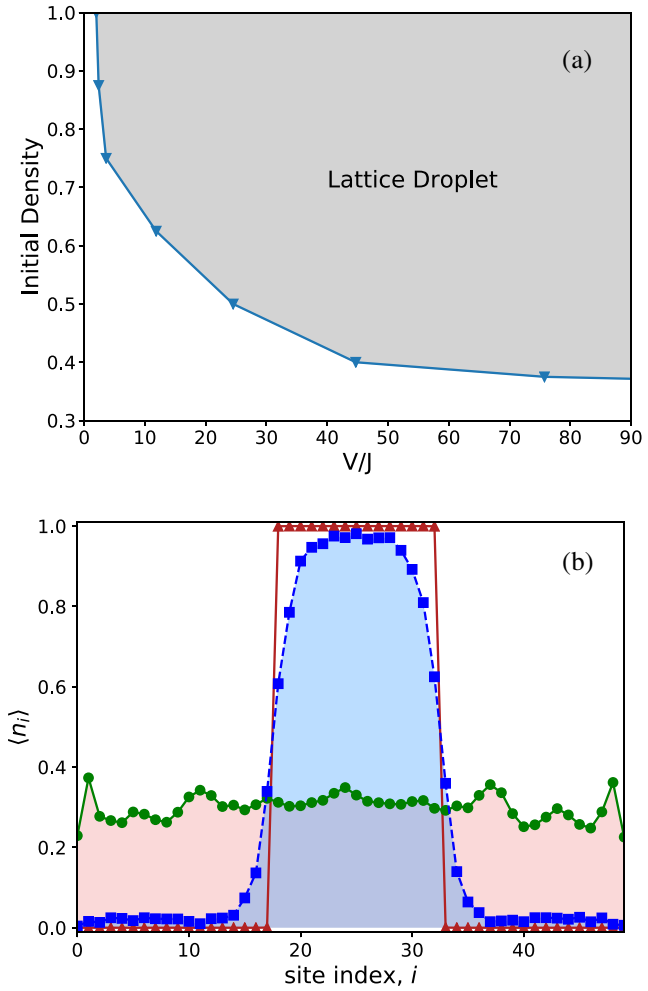

FIG. 3. (a) $(V/J)_{\rm cr}(\rho)$ for self-bound droplets obtained using exact evolution of Eq. (1) for 16 sites. The particles are initially in the ground state (with $V = 0$) of a box trap in the central 8 sites. We determine $F(V/J, \rho) = \xi(t_f)/\xi(0)$, where $\xi(t) = \rho_c(t) - \rho_{\rm av}$, with $\rho_{\rm av}$ the density for an homogeneous lattice gas, $\rho_c(t)$ the central density, and $t_f = 100 t_D$, with t_D the homogenization time for $V = 0$. We determine $(V/J)_{\rm cr}$ as that for which $F[(V/J)_{\rm cr}, \rho] = 0.1$. (b) Density distribution, obtained using t-DMRG simulations of Eq. (1) [40], for a gas initially confined with $\rho = 1$ (red triangles) $Jt = 30$ after release, for $V/J = 1$ (unbound, green circles) and $V/J = 2.5$ (droplet, blue squares).

Dimer clustering may then be probed in a few seconds, well within experimental lifetimes.

Lattice droplets.—Even much weaker DDI may dramatically impact the dynamics. We consider a hard-core gas at filling $\rho \leq 1$ initially prepared, with $V = 0$ (using the magic-angle orientation between dipole moment and lattice axis), in the ground state of a boxlike potential [49–51]. At time $t = 0$ the box trap is released and the dipole orientation is changed such that $V > 0$. In contrast to nonpolar experiments [21,22], where stable or partially stable on-site RBPs still allowed for an overall (slowed-down) expansion, in the polar case there is a critical $(V/J)_{\rm cr}(\rho)$ such that the cloud remains self-bound [Fig. 3(a)]. These self-bound

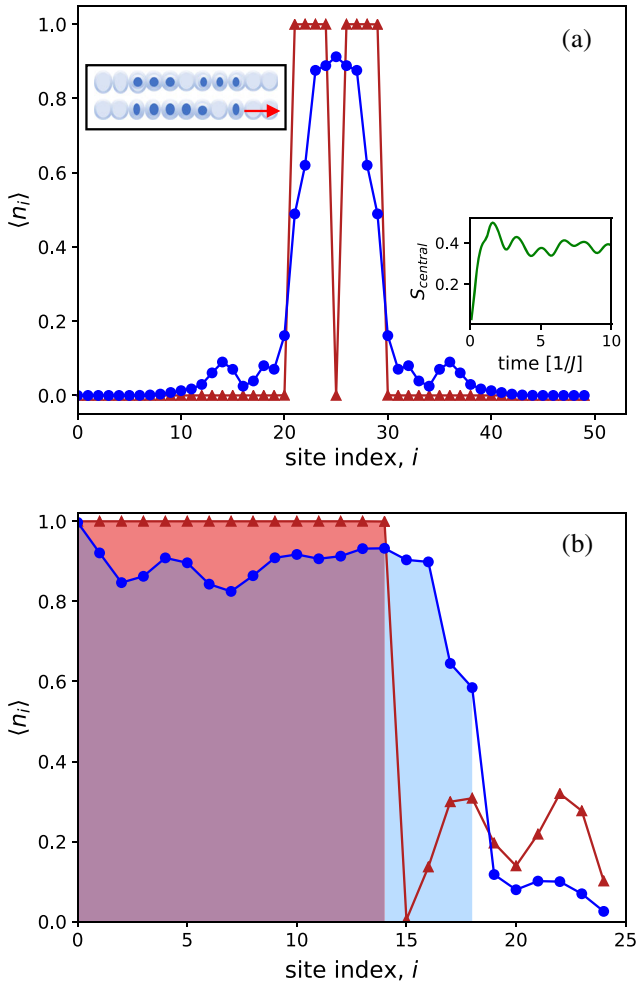

FIG. 4. (a) Droplet with a holon initially at the center (red triangles) after $Jt = 6$ (blue circles), for $V/J = 30$. Partial holon evaporation results in particle ejection (left inset), but is inefficient, as shown by the particle-hole entropy averaged over the 5 central sites (right inset). (b) Initial droplet with $\rho = 1$ and two singlons outside (red triangles) after $Jt = 55$ (blue circles). The shadowed region is that of the droplet. Note singlon aggregation at the droplet edge. Figures obtained by t-DMRG calculations using Hamiltonian (1) [40].

lattice droplets present a finite final average $\rho' < 1$ [Fig. 3(b)]; i.e., holons (empty sites) remain mobile but confined within a droplet. As a result, lattice droplets remain superfluid. For $\rho = 1$, droplets occur already for $V/J \simeq 2.5$. For current ^{166}Er experiments [27], with a lattice spacing of 266 nm and a typical lattice depth of 20 recoil energies, $V/J \simeq 2.7$, with a hopping time $1/J = 6.5$ ms.

For large-enough V/J, holons remain confined in the droplet due to the potential exerted by the droplet boundaries via the DDI tail. For $V/J \lesssim 8$ [Fig. 4(a)], this mechanism is insufficient, since only NN DDI are relevant. A holon, initially inside a droplet with $\rho = 1$, expands by resonant hops up to the edges. At that point, the last particle may escape without breaking any NN bond [left inset of Fig. 4(a)]. This holon evaporation becomes drastically inefficient for growing droplet sizes, since the holon quickly spreads uniformly within the droplet [right inset of Fig. 4(a)]. Therefore, holons remain confined within the droplet. The converse also occurs: a singlon may stick to the droplet edge, pushing a holon inside [Fig. 4(b)]. Mobile holons inside the droplet may be revealed using quantum gas microscopy.

Conclusions.—Polar gases in 1D lattices present a severely constrained dynamics. Dynamically bound dimers dramatically enhance the role of the dipolar tail, leading to quasi-localization in absence of disorder via dimer clustering even for low densities and moderate dipole moments. Moreover, polar gases may form, even for weak dipoles, self-bound superfluid lattice droplets. Our results hint at inherent difficulties in particle-hole entropy removal in polar lattice gases. Our work is directly relevant for current lanthanide experiments and future experiments with polar molecules, and may be easily extrapolated to other power-law interactions, $V/|i-j|^{\alpha}$ [52].

Our results may be extrapolated to higher dimensions. Whereas singlon-gluing just occurs in one dimension, since it requires singlon confinement between dimers, clusterization due to dimer-dimer DDI and self-bound lattice droplets occurs also in higher dimensions. For square lattices, L_{cr} is only slightly modified compared to 1D. The critical lattice filling for dimer localization via clustering scales, however, as $\rho_{cr} \simeq 1/L_{cr}$, and hence for moderate $V/J \sim 30$, $\rho_{cr} \lesssim 0.1$. Moreover, in contrast to 1D, when removing the overall confinement, but keeping the lattice on, singlons evaporate leaving an immobile dimer cluster behind despite the extremely dilute dimer density $\rho_D \simeq \rho_{cr}^2$ [53].

We thank L. Chomaz, F. Ferlaino, C. Menotti, M. Mark, T. Pfau, and A. Recati for discussions. W. L., X. D., and L. S. thank the support of the DFG (SFB 1227 DQ-mat and FOR2247), L. B. the ERC Starting Grant TopoCold, and K. K. the KAKENHI (Grant No. 18K03472) from the JSPS.

[1] A. Polkovnikov, K. Sengupta, A. Silva, and M. Vengalattore, Rev. Mod. Phys. **83**, 863 (2011).
[2] L. D'Alessio, Y. Kafri, A. Polkovnikov, and M. Rigol, Adv. Phys. **65**, 239 (2016).
[3] F. Borgonovi, F. M. Izrailev, L. F. Santos, and V. G. Zelevinsky, Phys. Rep. **626**, 1 (2016).
[4] D. M. Basko, I. L. Aleiner, and B. L. Altshuler, Ann. Phys. (Amsterdam) **321**, 1126 (2006).
[5] R. Nandkishore and D. A. Huse, Annu. Rev. Condens. Matter Phys. **6**, 15 (2015).
[6] I. Bloch, J. Dalibard, and W. Zwerger, Rev. Mod. Phys. **80**, 885 (2008).
[7] R. Blatt and C. F. Roos, Nat. Phys. **8**, 277 (2012).
[8] T. Kinoshita, T. Wenger, and D. S. Weiss, Nature (London) **440**, 900 (2006).
[9] M. Gring, M. Kuhnert, T. Langen, T. Kitagawa, B. Rauer, M. Schreitl, I. Mazets, D. A. Smith, E. Demler, and J. Schmiedmayer, Science **337**, 1318 (2012).

[10] P. Richerme, Z.-X. Gong, A. Lee, C. Senko, J. Smith, M. Foss-Feig, S. Michalakis, A. V. Gorshkov, and C. Monroe, Nature (London) **511**, 198 (2014).

[11] P. Jurcevic, B. P. Lanyon, P. Hauke, C. Hempel, P. Zoller, R. Blatt, and C. F. Roos, Nature (London) **511**, 202 (2014).

[12] M. Gärttner, J. G. Bohnet, A. Safavi-Naini, M. L. Wall, J. J. Bollinger, and A. M. Rey, Nat. Phys. **13**, 781 (2017).

[13] J. Billy, V. Josse, Z. Zuo, A. Bernard, B. Hambrecht, P. Lugan, D. Clément, L. Sanchez-Palencia, P. Bouyer, and A. Aspect, Nature (London) **453**, 891 (2008).

[14] G. Roati, C. D'Errico, L. Fallani, M. Fattori, C. Fort, M. Zaccanti, G. Modugno, M. Modugno, and M. Inguscio, Nature (London) **453**, 895 (2008).

[15] B. Deissler, M. Zaccanti, G. Roati, C. D'Errico, M. Fattori, M. Modugno, G. Modugno, and M. Inguscio, Nat. Phys. **6**, 354 (2010).

[16] S. S. Kondov, W. R. McGehee, J. J. Zirbel, and B. DeMarco, Science **334**, 66 (2011).

[17] F. Jendrzejewski, A. Bernard, K. Müller, P. Cheinet, V. Josse, M. Piraud, L. Pezzé, L. Sanchez-Palencia, A. Aspect, and P. Bouyer, Nat. Phys. **8**, 398 (2012).

[18] M. Schreiber, S. S. Hodgman, P. Bordia, H. P. Luschen, M. H. Fischer, R. Vosk, E. Altman, U. Schneider, and I. Bloch, Science **349**, 842 (2015).

[19] K. Winkler, G. Thalhammer, F. Lang, R. Grimm, J. Hecker Denschlag, A. J. Daley, A. Kantian, H. P. Büchler, and P. Zoller, Nature (London) **441**, 853 (2006).

[20] N. Strohmaier, D. Greif, R. Jördens, L. Tarruell, H. Moritz, T. Esslinger, R. Sensarma, D. Pekker, E. Altman, and E. Demler, Phys. Rev. Lett. **104**, 080401 (2010).

[21] U. Schneider *et al.*, Nat. Phys. **8**, 213 (2012).

[22] J. P. Ronzheimer, M. Schreiber, S. Braun, S. S. Hodgman, S. Langer, I. P. McCulloch, F. Heidrich-Meisner, I. Bloch, and U. Schneider, Phys. Rev. Lett. **110**, 205301 (2013).

[23] M. Saffman, T. G. Walker, and K. Mølmer, Rev. Mod. Phys. **82**, 2313 (2010).

[24] A. Browaeys and T. Lahaye, Interacting cold Rydberg atoms: A toy many-body system, in *Niels Bohr, 1913-2013*, Progress in Mathematical Physics Vol. 68, edited by O. Darrigol, B. Duplantier, J. M. Raimond, and V. Rivasseau (Birkhuser, Cham, 2016), pp. 177–198.

[25] A. de Paz, Phys. Rev. Lett. **111**, 185305 (2013).

[26] B. Yan, S. A. Moses, B. Gadway, J. P. Covey, K. R. A. Hazzard, A. Maria Rey, D. S. Jin, and J. Ye, Nature (London) **501**, 521 (2013).

[27] S. Baier, M. J. Mark, D. Petter, K. Aikawa, L. Chomaz, Z. Cai, M. Baranov, P. Zoller, and F. Ferlaino, Science **352**, 201 (2016).

[28] S. Ospelkaus, K.-K. Ni, D. Wang, M. H. G. de Miranda, B. Neyenhuis, G. Quemener, P. S. Julienne, J. L. Bohn, D. S. Jin, and J. Ye, Science **327**, 853 (2010).

[29] M. Mayle, G. Quéméner, B. P. Ruzic, and J. L. Bohn, Phys. Rev. A **87**, 012709 (2013).

[30] L. de Marco *et al.*, arXiv:1808.00028.

[31] T. Lahaye, C. Menotti, L. Santos, M. Lewenstein, and T. Pfau, Rep. Prog. Phys. **72**, 126401 (2009).

[32] M. Baranov, M. Dalmonte, G. Pupillo, and P. Zoller, Chem. Rev. **112**, 5012 (2012).

[33] M. Valiente and D. Petrosyan, J. Phys. B **42**, 121001 (2009).

[34] J.-P. Nguenang and S. Flach, Phys. Rev. A **80**, 015601 (2009).

[35] L. Barbiero, C. Menotti, A. Recati, and L. Santos, Phys. Rev. B **92**, 180406(R) (2015).

[36] For Fermi gases the droplets would remain metallic.

[37] The hard-core condition assumes strong on-site interactions, such that maximally one boson is allowed per site.

[38] Our results should not change qualitatively for single-component fermions.

[39] See Supplemental Material at http://link.aps.org/supplemental/10.1103/PhysRevLett.124.010404 for the details on the evaluation of the stability of NN dimers, the dimer-dimer states, and the dimer-singlon-dimer model.

[40] M. L. Wall and L. D. Carr, New J. Phys. **14**, 125015 (2012).

[41] The nature of the short-time plateaux of Fig. 2(a) is different for $V/J = 12$ and for $V/J = 42$. For $V/J = 12$, the atoms within the dimers are not fully rigidly bound at nearest neighbors, but rather have small probability to separate to next-nearest neighbors. This slight spreading explains the entropy growth for $t \sim 1/J$. This initial growth is followed by a plateau, because any further entropy growth demands the dimer motion, which occurs at $t \sim 1/J_D \gg 1/J$. This entropy growth then proceeds unhindered since no dimer cluster forms. For $V/J = 42$ the dimers are rigidly formed by nearest-neighbor atoms, and hence entropy growth at the $1/J$ timescale is prevented. The small entropy growth at $t \sim 1/J_D$ is due to the slightly undefined relative interdimer distance having a finite variance $\Delta L \ll L_0$. That growth of $S(t)$ is followed by a plateau, since further entropy growth demands the motion of the whole dimer-dimer cluster, which occurs in a longer timescale.

[42] $S_{\max}$ may be determined from the dimension of the energetically available Hilbert manifold D, as $S_{\max} = \log(D)$. For the case of two freely moving dimers, $D \simeq N_s^2$, whereas for bound dimers at a rigid fixed distance, $D \simeq N_s$. Similarly for two dimers with a singlon in between, $D \simeq N_s^3$ if the dimers and the singlon move freely. For bound dimers at a fixed distance L with a freely moving singlon in between, $D \simeq N_s L$. Finally, if the singlon position is pinned at the center of the two dimers, $D \simeq N_s$.

[43] D. Petrosyan, B. Schmidt, J. R. Anglin, and M. Fleischhauer, Phys. Rev. A **76**, 033606 (2007).

[44] Note that dimers remain at a fixed distance for all initial separations $L < L_{\rm cr}$. As a result, multidimer clusterization does not require an initial dimer crystal, i.e., the distance between neighboring dimers in the cluster may be in general unequal.

[45] Because of periodic boundary conditions, a single singlon, which may present different winding numbers around the periodic system, will lead to Brownian motion of the NNDs, mimicking the behavior expected for NNDs in a singlon bath.

[46] T. Grover and M. P. A. Fisher, J. Stat. Mech. (2014) P10010.

[47] M. Schiulaz, A. Silva, and M. Müller, Phys. Rev. B **91**, 184202 (2015).

[48] We consider neither nearest-neighbor clusters of $n > 2$ particles, which occur with density ρ^n, nor the formation of dimers beyond nearest neighbors. For sufficiently large V/J these dimers may become stable as well. Their presence, however, would result in an even stronger localization of the lattice gas.

[49] More general confinements, e.g., harmonic traps or finite-temperature effects do not modify our conclusions.
[50] The hard core condition may be easily imposed by setting a large value for the scattering length using Feshbach resonances.
[51] V depends as $(1-3\cos^2\theta)$, with θ the angle between the dipole moment and the lattice axis. Hence, in one dimension $|V|$ can be changed all the way from its maximal value to zero. The latter occurs at the so-called magic angle, $\theta_M = \arccos(1/\sqrt{3})$.
[52] For a power α, the critical interdimer distance for dimer clustering scales as $L_{\mathrm{cr}} \propto (V/J)^{2/\alpha}$.
[53] This must be compared to clusters of nonpolar RBPs resulting from quantum distillation [43] which occur at a unit filling of pairs.